# Durability Analysis on Solar Energy Converters containing Polymeric Materials

Jochen Wirth*, Steffen Jack, Michael Köhl and Karl-Anders Weiß
Fraunhofer Institute for Solar Energy Systems ISE, Heidenhofstrasse 2, 79110 Freiburg, Germany
*Mail: jochen.wirth@ise.fraunhofer.de

**Abstract:** The key issues of the Fraunhofer Institute for Solar Energy Systems are research and development of solar technologies for the fast growing market of solar energy. This paper presents examples of the usage of *COMSOL Multiphysics*:
The ingress of water is a serious reason for the degradation of photovoltaic modules which can hardly be measured using experimental approaches yet. Therefore, a modeling approach was used regarding the water ingress under different climatic conditions as well as variations of the design of the PV module.
Further on, the issues of efficiency, thermo-mechanical and external loads of polymer solar thermal flat plate collectors have been examined.

**Keywords:** photovoltaic modules, permeation, polymer flat plate collectors, thermo-mechanical loads

## 1 Introduction

Polymeric materials are used as water vapour barriers or encapsulation materials for photovoltaic modules. Further, the development of polymer flat plate solar thermal collectors is enforced by not only substituting common materials but reengineering the collector optimised for properties of polymer materials. Both applications have to reach a service life time of more than 20 years. Therefore, numeric simulations are used in different stages of development in order to gain knowledge on durability.

Little long time experience on degradation processes of photovoltaic modules caused by mass transport of water inside the module is available. Therefore, research is carried out to further ensure the predicted service life time of these applications.

Durability analysis and efficiency calculations can be performed by numeric simulations in order to identify problems and options for the recently started development of solar thermal flat plate collectors based on polymers before building a prototype collector.

### 1.1 Mass Transport of Water within Photovoltaic Modules

A serious reason for degradation of photovoltaic modules is the ingress of water which can cause corrosion and degradation of functional properties. [1.4] The permeation properties of polymeric encapsulation materials determine the amount of water in the polymers and inside the modules. The temperature of solar modules and the ambient water vapour concentration vary over time according to the solar radiation and the ambient climate. Temperature-dependent permeation and diffusion properties are needed for modelling the water concentration over time to predict the long-term behaviour and the service life of such devices.

In this regard, mass transport of water inside the module was simulated using *COMSOL Multiphysics*. A variety of different ambient conditions and module component materials were considered for simulation in order to determine the various influences. Further variations were performed for the encapsulation material and by using climates of different sites like Freiburg in Germany, Ny Ålesund in Norway or Momote in Papua New Guinea.

### 1.2 Calculation of thermo-mechanical Loads on Polymer Collectors

Regarding flat plate solar thermal collectors made of polymers, the overall geometry has to be optimised for considered materials. Due to the low thermal conductivity the contact area between absorber layer and fluid has to be maximised. [1.8] To be able to use low cost processes like extrusion, specific geometrical constraints have to be considered. As a first step, numerical

simulation is used to compare different collector geometries regarding the fluid dynamics and the possible positions of the absorber layer. The efficiency has been calculated for different system parameters like flow rate and geometry.

The temperature distributions during operation and stagnation are used as input parameters for numerical simulation of mechanical stresses due to thermal expansion. External loads like snow load are examined as well. By varying material combinations and geometries the resulting stress distribution and deformation display potential risks concerning the stability and durability of the collectors.

## 2 Material Parameters

A common Photovoltaic Module was considered for the simulations (Figure 2.1). It consists of a front glazing, a back sheet, and an encapsulation material in which solar cells are embedded. For the material of the glazing a glass cover with a thickness of 3200 µm was used. A 150 µm PVF-PET-PVF layer was used as the back sheet cover. Between these covers in the front and in the back of the Si solar cell Ethylene-Vinylacetate (EVA) encapsulation material layers (33 % VA) with thicknesses of 450 µm each were assumed. The 200 µm thick Si solar cells with a length and width of 6" = 15.24 cm were situated next to each other in a distance of 3 mm.

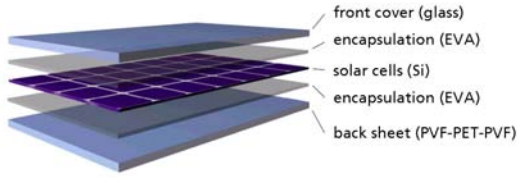


**Figure 2.1.** Common design of a photovoltaic module.

The presented flat-plate collector is rather distinct from conventional collector types due to selecting a design physique that enables a large number of collector components to be embedded in one structural element. In addition, the heat transfer fluid is circulated through the complete absorber area to achieve high collector efficiency. Figure 2.2 illustrates the collector geometry as well as a cross cut through the simulation model.

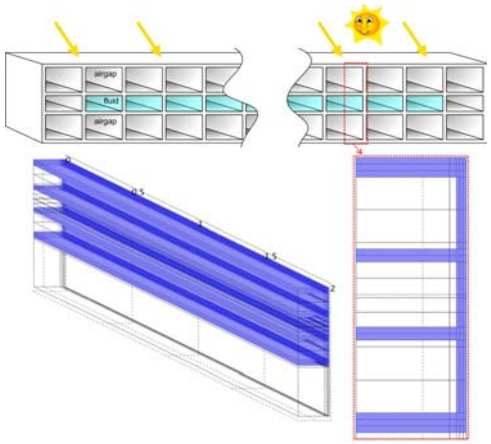

**Figure 2.2.** Polymer flat plate collector and simulation model of half a fluid channel.

## 3 Boundary Conditions and Governing Equations

### 3.1 Mass Transport of Water within Photovoltaic Modules

#### 3.1.1 Temperature of the Silicon Solar Cell

Solar irradiation causes significant heating, especially of the silicon components, whereas wind effects cause cooling of the module. On sunny days, the temperature inside the module is clearly higher than the ambient temperature. Since the heating processes of the module are very complex, an approximation is used to describe the cell temperature. [1.6] Using

$$T_{\text{cell}} = T_{\text{amb}} + \frac{H}{U_0 + U_1 \cdot v} \qquad (3.1)$$

the temperature of the solar cells $T_{\text{cell}}$ in the PV module depends on the ambient temperature $T_{\text{amb}}$, on the solar radiation $H$, and on the wind velocity $v$. $U_0$ and $U_1$ were determined by evaluating measurements of different areas. Simplifying equation 3.1 and assuming a constant wind velocity of 1 m/s, the following estimation was used in the models for describing the cell temperature:

$$T_{\text{cell}} = T_{\text{amb}} + \frac{7}{200}\frac{Km^2}{W} H \qquad (3.2)$$

Using this boundary condition for cell temperature, the temperature distribution and the heat transfer inside the glass and different polymeric parts of the PV module was simulated using the heat transfer module of *COMSOL*

*Multiphysics*. This is needed for calculating the temperature dependent diffusion coefficient which is described in paragraph 3.1.2.

### 3.1.2 Diffusion Coefficients

The diffusion coefficients are the most important variables for the simulation of the water transport inside the PV module. Therefore, it is important to know their properties in the simulations as precisely as possible. Most important hereby are their dependence on the temperature and the concentration of water in the polymers. At a temperature of $T = 300$ K the diffusion coefficients in dry polymers are

$$D_{\mathrm{EVA}} = 8{,}7 \cdot 10^{-11} \frac{m^2}{s} \qquad (3.3)$$

for the EVA encapsulation material and

$$D_{\mathrm{bs}} = 7{,}4 \cdot 10^{-12} \frac{m^2}{s} \qquad (3.4)$$

for the PVF-PET-PVF back sheet. [1.1]

It is assumed that glass and Silicon do not absorb any water, therefore their diffusion coefficients are

$$D_{\mathrm{Si}} = D_{\mathrm{glass}} = 0 \frac{m^2}{s} \qquad (3.5)$$

The temperature dependence of the diffusion coefficient is assumed to follow the law of *Arrhenius*. [1.7]

Thus, the diffusion coefficient at a temperature $T$ at a specific point inside the module is

$$D(T) = D_{T_0} e^{\frac{E_{\mathrm{D}}}{\mathrm{R}}\left(\frac{1}{T_0} - \frac{1}{T}\right)} \qquad (3.6)$$

with $D_{\mathrm{T0}}$ as the diffusion coefficient at temperature $T_0$, and $E_{\mathrm{D}}$ as the activation energy of the diffusion for the specific material. R is the gas constant.

The concentration dependency of the diffusion coefficient $D$ at a specific concentration $c$ can be determined by

$$D(c) = D_0 \cdot e^{\gamma \cdot c} \qquad (3.7)$$

with $D_0$ as the diffusion coefficient of a dry polymer, $E_{\mathrm{D}}$ as the activation energy of diffusion, and $\gamma$ as the plastification coefficient. [1.3]

## 3.2 Calculation of thermo-mechanical Loads on Polymer Collectors

Solar thermal collectors as energy converters of solar irradiation into heat should convert as much irradiation into useful heat as possible, in contrast to PV-modules. To do so, the collector should have a high thermal efficiency and be durable against thermo-mechanical loads as well as external mechanical loads.

### 3.2.1 Heat Transfer and Efficiency

The cover of the solar collector should transmit as much solar irradiation as possible which should then be absorbed by the selective coating of the absorber. Thus, the power arriving at the absorbing layer $\dot{Q}_{\mathrm{abs}}$ is

$$\dot{Q}_{\mathrm{abs}} = I - \dot{Q}_{\mathrm{loss,opt}} = I \cdot \tau_{\mathrm{front}} \cdot \alpha_{\mathrm{abs}} \qquad (3.8)$$

with the irradiance $I$ in W/m², the transmittance $\tau$ and the absorptance $\alpha$. A certain amount of heat is lost to the ambience by radiation and convection effects described by $\dot{Q}_{\mathrm{loss,therm}}$. The remaining part is transferred to the heat transfer fluid and is equal to the effective power output

$$\dot{Q}_{\mathrm{use}} = I - \dot{Q}_{\mathrm{loss,opt}} - \dot{Q}_{\mathrm{loss,therm}} . \qquad (3.9)$$

Throughout the simulation it is thus possible to determine the collector efficiency $\eta$ at different operating conditions:

$$\eta = \frac{\dot{Q}_{\mathrm{use}}}{I} = \frac{\dot{m} \cdot c_p \cdot \Delta T}{\dot{Q}_{\mathrm{use}} + \dot{Q}_{\mathrm{loss,opt}} + \dot{Q}_{\mathrm{loss,therm}}} \qquad (3.10)$$

with the mass flow rate $\dot{m}$ in kg/s, the specific heat capacity $c_{\mathrm{p}}$ of the transfer fluid in J/kgK and the temperature difference $\Delta T$ between the fluid inlet and outlet in K. [1.5] With

$$\dot{Q}_{\mathrm{use}} = U_{\mathrm{int}} \cdot \left(T_{\mathrm{abs}} - T_{\mathrm{fluid}}\right) \qquad (3.11)$$

it is possible to use the internal conductance $U_{\mathrm{int}}$ for an evaluation of the heat transfer abilities of the absorber geometry and the fluid flow under laminar flow conditions.

The heat transfer coefficient was used as boundary condition which offers sufficiently exact results concerning collector efficiency and temperature distributions to account for the thermal convective losses inside the air gap and between collector and ambience. The radiation losses have been considered by setting surface-to-surface and surface-to-ambient boundary conditions.

Altogether, with the HT-module it is possible to determine heat transfer abilities of the absor-

ber, total solar thermal collector efficiencies and the occurring temperature levels with differing geometry parameters, materials and surrounding parameters. All accomplished simulations are steady state analyses.

### 3.2.2 Thermo-mechanical Loads

The temperature distributions under various operating conditions which have been determined by the HT-module are used within the SM-module to evaluate the thermo-mechanical loads inside a collector. The temperature gradient in the components causes an uneven expansion of the material which results in deformations and stresses in the collector. Material combinations, material's thicknesses and characteristics have been varied to determine the influence of geometries and materials on the deformations and stresses inside the collector.

In addition to the 3D-model in Figure 2.2 a 2D-Model was generated which allows the assessment of the expansions perpendicular to the flow channels. The maximum allowed expansion $\sigma_{valid}$ was set to be

$$\sigma_{valid} = \frac{\sigma_{0,2\%}}{2} \cdot \left[1 - \left(k \cdot (T - 20)\right)\right] \cdot \frac{1}{1{,}3} . \quad (3.12)$$

The reduction factor $k$ describes the temperature dependence of the 0.2%-yield stress $\sigma_{0.2\%}$. Other commonly used safety and reduction factors are part of the upper equation.

Table 2.1 shows the polymeric materials that have been considered in the simulation series.

**Table 4.1.** Potential polymers for the use in polymer collectors

| Polymer | Optical properties | Heat conductivity in W/mK | Max. operating temp. in °C |
|---|---|---|---|
| PMMA | transparent | 0.19 | 75-90 |
| PC | transparent | 0.21-0.24 | 130 |
| PE-HD | translucent | 0.42-0.43 | 80-90 |
| PP | translucent | 0.22 | 90-100 |
| POM-C | opaque | 0.31 | 90 |
| PPS | opaque | 0.25 | 180-200 |
| PPO | opaque | 0.19-0.22 | 105 |

Next to the simulations of thermo-mechanical loads external loads were evaluated, too. During winter heavy snow fall can lead to big external loads and mechanical stresses. These have to be tolerated by the collector. Loads of 1000 Pa vertically to the collector should only cause deformation ≤ 0.5 %. [1.2] Within this simulation series the material's thickness and the channel width of the absorber have been varied to determine the geometric characteristics at which the maximal valid deformation occurs.

## 4 Numerical Results

### 4.1 Mass Transport of Water within Photovoltaic Modules

### 4.1.1 Variation of Climatic Conditions

For the models, climatic parameters were used which had been measured every five minutes for one year at different locations. Data of temperature $T$, relative humidity $\varphi$ (which was transformed into absolute humidity using the *Magnus* Formula), and solar radiation $H$ were used from the climatic conditions of Freiburg in Germany, Miami in Florida, USA, Riyahd in Saudi Arabia, Ny Ålesund in Norway and Momote on Manus Island, Papua New Guinea.[1.9]

Figure 4.1 shows the water concentration inside the module after five days, Figure 4.2 after one year for the module being exposed to the climatic conditions of Freiburg in Germany starting in March.

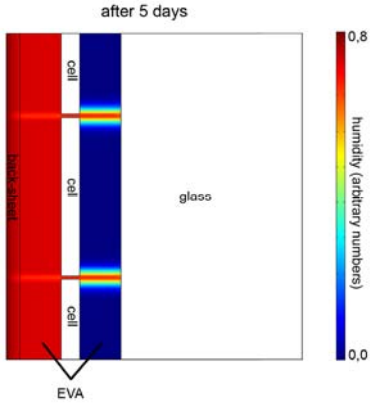


**Figure 4.1.** Simulation of the spatial distribution of water inside the PV module after five days. The humidity from the ambience reached the encapsulation material between back-sheet and cell and a small region between cell and glazing close to the gap between two cells after five days.

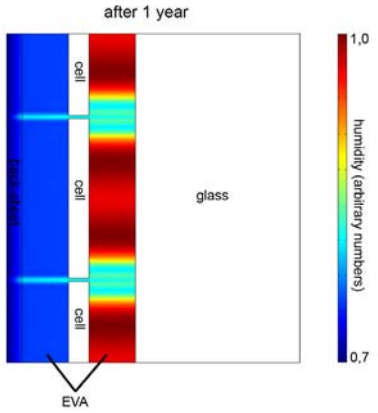


**Figure 4.2.** After one year, the highest calculated humidity level is between cell and glazing while the encapsulation material near the back-sheet has dried out during winter times (B). The humidity was very low during the last 150 days (Nov.–March) which caused the drying of the EVA near the back-sheet.

The development of the water concentration inside the module over five years is shown in Figure 4.3. The simulations show that it takes about 50 days until water reaches all points of the encapsulation material of the module for Freiburg, Germany. The maximum water concentration inside the module is reached after four years.

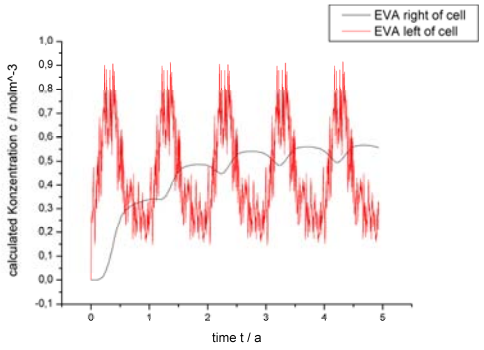


**Figure 4.3.** Simulation results: The concentration of water in a module between the glazing and the PV-cell (right of cell) compared to its concentration on the opposite side (left of cell) at the level of the centre of the cell during five years is shown for Freiburg.

Significant differences were found for the other mentioned climates (Figure 4.4). It takes only 20 days in Momote, while it takes up to 200 days in Spitzbergen until the humidity reaches all regions of the encapsulation material. In the same way, the maximum concentration reached at the analysed point differs between 0.017 mol/m³ for Spitzbergen and 0.945 mol/m³ for Momote.

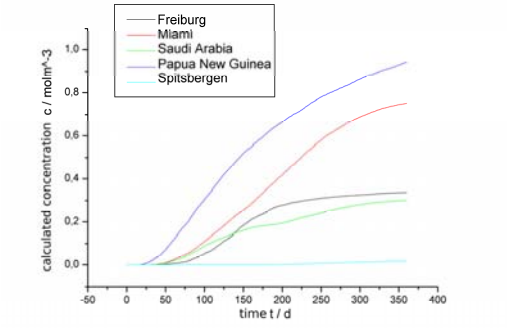


**Figure 4.4.** Simulation results: Comparison of the concentration of water near the cell under different climates.

### 4.1.2 Variation of Encapsulation and Back Sheet Materials

An parameter sensitivity study for the diffusion coefficient was performed for variations of the encapsulation and back sheet materials. The results (Figure 4.5) show that the variation of the diffusion coefficient of the encapsulation material does have a strong influence on the humidity conditions in the module while the variation of the diffusion coefficient of the back sheet material only has an insignificant influence.

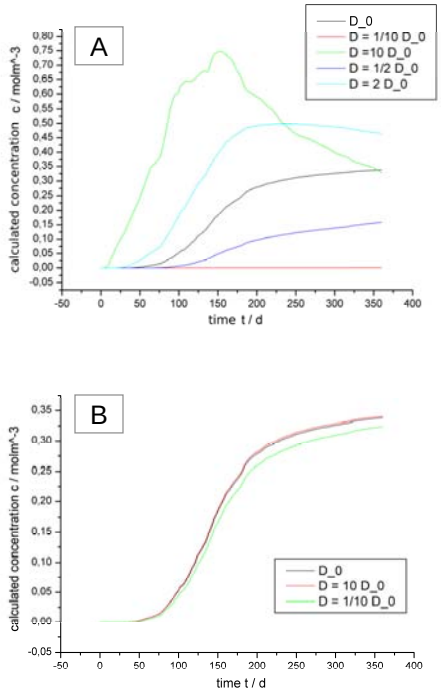


**Figure 4.5.** Simulation results: Concentration of water in a module between the glazing and the PV-cell above the centre of the cell during one year. Parameter sensitivity studies of the diffusion coefficients of the encapsulation materials (A) and of the diffusion coefficient of the back sheet material (B) with $D\_0 = 8.7 \cdot 10^{-7}$ m²/s. Both simulations used yearly climatic data starting in March.

## 4.2 Calculation of thermo-mechanical Loads on Polymer Collectors

### 4.2.1 Heat Transfer to the Fluid and Collector Efficiency

The fluid flow inside the absorber channel was calculated to determine the internal conductance. Figure 4.6 shows cross sections of the flow profiles for different collector geometries.

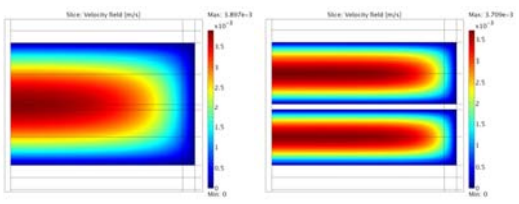

**Figure 4.6.** Fluid flow profile for a full absorber channel and a divided absorber channel with a dividing absorbing plate.

An absorber geometry with full channel and absorption on top with material thickness of 2 mm leads to an internal conductance of 95 W/m²K whereas absorption at the bottom of the channel, leads to a conductance of 190 W/m²K. Using an absorption plate in the middle of the channel it was possible to increase the internal conductance to 540 W/m²K.

Looking at the complete collector following efficiencies were found (Figure 4.7).

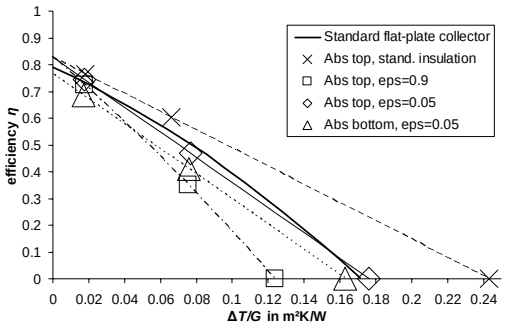


**Figure 4.7.** Collector efficiencies depending on the temperature difference between fluid and ambience for a standard flat plate collector and variations of the regarded polymer collector; An air gap as back insulation and a high emission on the back of the absorber increase thermal losses. An absorption at the bottom inside the absorber channel increases optical losses.

It became apparent that the emissivity of the absorber surface is a key factor to the thermal losses for a. Further, the conversion factor (ordinate-intercept) of the collector with absorption inside the channel is lower due to the additional plate, which increases the optical losses.

### 4.2.1 Thermo-mechanical Loads and External Loads

The uneven expansion of the homogeneous material is due to the temperature gradients in the components. Figure 4.8 illustrates the temperature distributions for different collector operating conditions.

The resulting deformations and Von Mises stress distributions are shown exemplarily in figure 4.9 for certain geometries and materials.

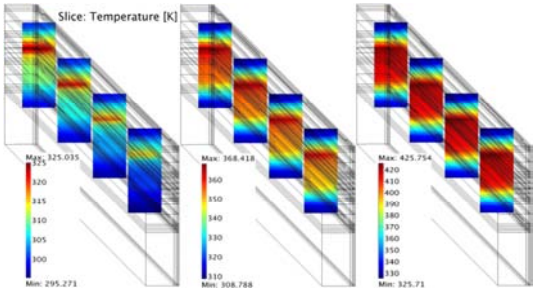


**Figure 4.8.** Temperature distribution of a 2 m long fluid channel with absorbing surface on top of the absorber for inlet temperatures of 300 and 350 K (left and middle) and stagnation (right)

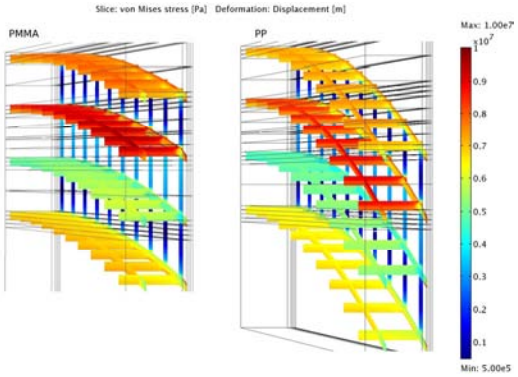


**Figure 4.9.** Von Mises stress distribution and Deformation of the 2 m long collector model with a wall thickness of 2 mm at a inlet temperature of 350 K

The calculated max. stresses for these simulation models are always below the defined max. valid stress (equation 3.12). Using PMMA as collector material the max. deformation at the outlet of the fluid channel shows about 20 mm of displacement, which equals a bending of one percent for a collector length of two meters. This does not affect the usability of the collector but displays an obvious deformation. The collector configurations with a combination of two materials show a considerably larger deformation due to the different thermal expansion coefficients of the materials.

Within the simulation set using the 2D-model which describes the collector crosswise to the fluid channels the deformations are lower than determined by the 3D-model. The max. calculated stresses are higher. In figure 4.10. the max. occurring stresses are displayed for various material's thicknesses and materials.

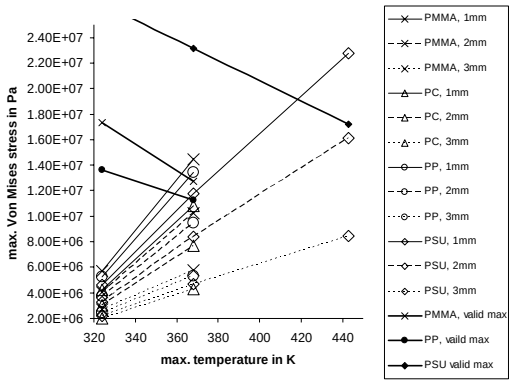


**Figure 4.10.** Max. Von Mises stress for different polymers and material thicknesses in the 2D-collector model crosswise to the fluid channels depending on operating temperature; For a wall thickness of 1 mm the max. stress reaches values higher than the estimated max. valid stress.

It indicates clearly that the collector shows different mechanical characteristics in the direction of the fluid channels and crosswise to them. The complexity of the entire collector geometry does not allow examination of the complete collector. The summation of the position depending stresses from both model types exhibits stress values below the defined max. valid stresses for most of the considered configurations.

The analysis regarding the snow load shows that the stability of the collector is given for most of the considered geometry parameters at a top pressure of 1000 Pa. Figure 4.11 shows exemplary the stress distribution and the 30x scaled deformation.

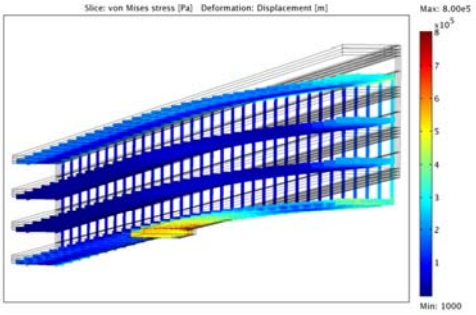


**Figure 4.11.** Von Mises stress distribution and Deformation (scaled 30x) due to 1000 Pa top load for a collector model with 2 mm wall thickness and PP as material

## 5 Conclusion

The modelling of mass transport of water inside photovoltaic modules can give important information on module degradation which can support complicated experimental approaches. It was shown that the mass transport of water within PV modules depends strongly on the climatic conditions of the environment. For the regarded climates, it takes between 20 and 200 days for the humidity to reach all points of the encapsulation. While the variation of the diffusion coefficient of the encapsulation material has a strong influence on the humidity conditions in the module, the diffusion coefficient of the back sheet material is insignificant.

The studies conducted on polymeric collectors confirm that by circulating the heat transfer fluid through the complete absorber area it is possible to reach heat transfer characteristics similar or even higher than in conventional absorbers.

The thermo-mechanical loads in the considered collector geometry causes deformations during collector operation which should not be neglected. The deformations are even larger when using two different polymeric materials which are joined together because of the different thermal expansion. The external loads considered do not cause any comparable stresses in the collector geometry.

The optimised polymeric collector geometry has a similar efficiency as a conventional collector and the mechanical stability is sufficient when the collector is constructed correctly.

## 6 Acknowledgements

The work was partly funded by the German Federal Ministry of Education and Research (BMBF FKz: 01RI05201) and the German Federal Ministry for the Environment, Nature Conservation and Nuclear Safety (BMU FKz 0329978).

## 7 References

[1.1] Bregulla, M.; Köhl, M.; Lampe, B.; Oreski, G.; Philipp, D.; Wallner, G.; Weiß, K.-A.: *Degradation Mechanism of Ethylen-Vinyl-Acetate Coplymere - New Studies including Ultra Fast Cure Foils.* Milano : PVSEC, 2007

[1.2] CEN: *EN 12975-2:2006 (E), Thermal Solar Systems and Components, Solar Collectors, Part 2: Test Methods*. Juni 2006

[1.3] Crank, J.: *The Mathematics of Diffusion*. Oxford : Oxford University Press, 1975

[1.4] Czanderna, A.W.; Pern, F.J.: *Encapsulation of PV modules using ethylene vinyl acetate copolymer as a pottant: A critical review.* In: *Solar Energy Materials and Solar Cells Vol. 43*, Page 101-181, 1995

[1.5] Duffie, John; Beckman, William: *Solar Engineering of Thermal Processes.* 3. edition, Hoboken, New Jersey : John Wiley & Sons, 2006

[1.6] Faiman, D.: *Assessing the Outdoor Operating Temperature of Photovoltaic Modules.* Prog. Photovolt: Res. Appl. 2008; Vol. 16, Page 307–315, 2007

[1.7] Kempe, M.D.: *Modeling of rates of moisture ingress into Photovoltaic modules.* In: *Solar Energy Materials and Solar Cells Vol. 90*, Page 2720-2738, 2006

[1.8] Rommel, Matthias; Moock, Wolfgang: *Collector Efficiency Factor F` for Absorbers with Rectangular Fluid Ducts Containing the Entire Surface.* In: ISES (Ed.): *Solar Energy, Vol. 60.* Page 199-207, 1997

[1.9] World Radiation Monitoring Center, Institute for Atmospheric and Climate Science, ETH Zürich (Ed.): *Baseline Surface Radiation Network.* 2007